pISSN 1229-3008 eISSN 2287-6251
Progress in Superconductivity and Cryogenics
Vol.19, No.2, (2017), pp.38~43 https://doi.org/10.9714/psac.2017.19.2.038

Conceptual design of cooling anchor for current lead on HTS field coils

C. J. Hyeon[a], J. H. Kim[a], H. L. Quach[a], S. H. Chae[a], Y. S. Yoon[b], J. Lee[c], S. H. Han[c], H. Jeon[c], Y. H. Choi[d], H. G. Lee[d], and H. M. Kim[*, a]

[a] *Department of Electrical Engineering, Jeju National University, Jeju, S. Korea*
[b] *Department of Electrical Engineering, Shin Ansan University, Ansan, S. Korea*
[c] *Department of Electrical and Electronic Engineering, Yonsei University, Seoul, S. Korea*
[d] *Department of Materials Science and Engineering, Korea University, Seoul, S. Korea*

(Received 22 March 2017; revised or reviewed 2 May 2017; accepted 3 May 2017)

Abstract

The role of current lead in high-temperature superconducting synchronous machine (HTSSM) is to function as a power supply by connecting the power supply unit at room temperature with the HTS field coils at cryogenic temperature. Such physical and electrical connection causes conduction and Joule-heating losses, which are major thermal losses of HTSSM rotors. To ensure definite stability and economic feasibility of HTS field coils, quickly and smoothly cooling down the current lead is a key design technology. Therefore, in this paper, we introduce a novel concept of a cooling anchor to enhance the cooling performance of a metal current lead. The technical concept of this technology is the simultaneously chilling and supporting the current lead. First, the structure of the current lead and cooling anchor were conceptually designed for field coils for a 1.5 MW-class HTSSM. Then, the effect of this installation on the thermal characteristics of HTS coils was investigated by 3D finite element analysis.

Keywords: Conduction cooling, Cooling anchor, Current lead, HTS synchronous machine, Neon

1. INTRODUCTION

In general high-temperature superconducting synchronous machines (HTSSM) equipped with HTS coils as field windings of the rotor part, connecting the HTS field coils at cryogenic temperature with the external power supply unit at room temperature using a current lead is electrically and physically essential to charge the HTS field coils and compensate the magnetic flux of the field coils during operation mode. Thus, heat transfer caused by thermal conduction and Joule-heating losses to the HTS field coils is inevitable.

In [1-3], the thermal losses through the current lead were reported to be 15 %, 19 %, and 28 % of the total rotor losses in cases of a 10-MW-class HTS wind generator and 3- and 1.5-MW-class HTS ship propulsion motors, respectively. Such heat can increase the cooling load of a cryocooler for the rotor part of HTSSMs and decrease thermal-stability in the HTS coils, which means that the temperature in the heated HTS coils rises. Despite the introduction of thermal-anchoring technique that connects current lead and cryogenic structure of the rotor and can reduce heat-transfer losses such as conduction (Q_c) and Joule-heating (Q_j) losses, the highest temperature in HTS coils are always generated around the junction joining the HTS coils and current lead [4].

Therefore, a novel cooling technique is needed to quickly and smoothly cool down the current lead. In this pa-per, we present a novel concept of cooling anchor for a copper (Cu) current lead. The technical concept of the cooling anchor is the simultaneously chilling and supporting the current lead resulting from the direct coupling of the current lead with the cryogen return pipelines inside the HTSSM rotor. Thus, the cooling anchors can minimize heat intrusion toward the HTS field coils because it can prevent overheating of the current lead by conduction cooling from the returning cryogen. Technically, the difference of this device compared with the conventional thermal-anchoring technique is the use of the returned gas neon (GNe) as a cooling source.

This study focuses on the conceptual design of a Cu current lead with cooling anchors for a 1.5-MW-class HTSSM, and their thermal characteristic analysis, which considers two cases i.e., before and after the application of a cooling anchor, has been conducted by 3D electromagnetic and thermal finite element method (FEM). Finally, the Cu current lead structure was optimized based on the thermal FEM analysis results.

2. CONCEPTUAL THERMAL DESIGN OF A ROTOR

2.1. Design of conventional Cu current lead

To conceptually design the basic structure of the Cu current lead for 1.5-MW-class HTSSM field coils, which is conduction-cooled by the cryogenic end part, i.e., the HTS

* Corresponding author: hmkim@jejunu.ac.kr

coil side, an approximate differential equation in a steady-state thermal-transfer unit lead length was used as the governing equation for the conduction-cooled current lead, which is expressed as follows [1, 5]:

$$Q_l = Q_c + Q_j = \left(k(T)A\frac{dT}{dz} + \rho(T){I_{op}}^2 \frac{dz}{A} \right)\Big|_{z=l} \quad (1)$$

where Q_l is total heat loss at the cryogenic end part (approximately 30 K) of the current lead, which consists of Q_c and Q_j expressed by the first and second terms at the right-hand side, respectively. T and A are the temperature and cross- sectional area of the lead at $z = l$, respectively. l is the current lead length and assumed to be approximately 1.025 m considering the shaft design. As material properties, $k(T)$ and $\rho(T)$ are the thermal conductivity and electrical resistivity, respectively, of Cu at T. The operating current (I_{op}) of the HTS coils flowing through the current lead was set at 315 A in this design. Finally, Q_l simultaneously changes with the variation in the lead diameter (d), which determines A and is the final parameter that we need to optimize [5].

Fig. 1 shows the relationships of the heat loss versus variable diameter of the Cu current lead with its schematic view. Structurally, optimal d of the Cu current lead to minimize Q_l was estimated by analytical method, and its value was 8.3 mm based on a temperature range from 27 to 300 K, where the corresponding Q_l value was 18.43 W with Q_c = 9.17 W and Q_j = 9.26 W. On this occasion, the total Q_l value for one pair of Cu current lead was 36.86 W.

Fig. 2 shows the current density and Joule-heating loss density distribution in the Cu current lead computed by MAXWELL 3D electromagnetic FEM software. The calculated Q_j value was 9.85 W. The difference in the Q_j value compared with that from the analytical calculation method comes from the changes in the FEM geometry design, which may have changed the current density in each part of the current lead.

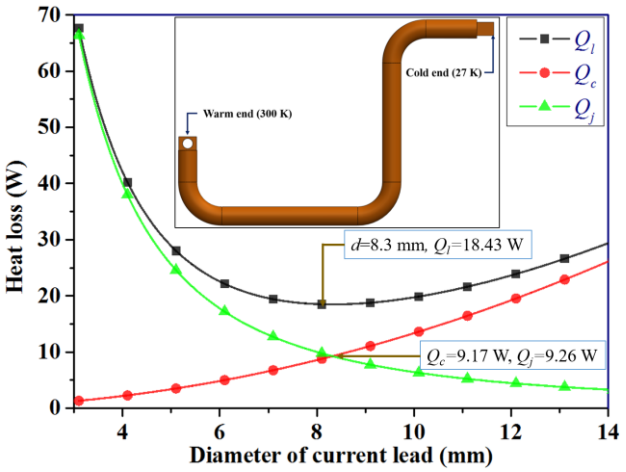

Fig. 1. Variations in heat loss versus diameter d of the Cu current lead.

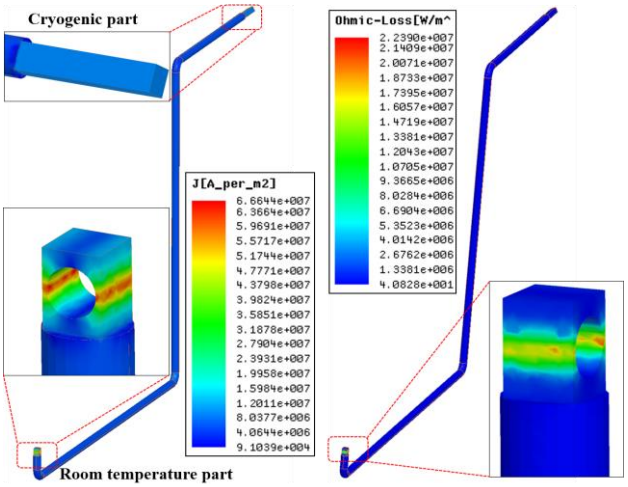

Fig. 2. Current density and Joule-heating loss distribution in the Cu current lead.

2.2. Design of rotor cooling system with cooling anchor

Fig. 3 shows the configuration of a cryogenic cooling system with the application of the cooling anchor concept for a 1.5-MW-class HTSSM, which has been conceptually designed from [3, 6], and [7]. The forced-circulation cooling technique using a closed-loop-type cooling pipe and a cryogen pump was adopted as the rotor-cooling method. The basic cooling scheme expresses that liquid cryogen, e.g., liquid neon (LNe), is supplied and circulates inside the bobbin block of the HTS field coils through the cryogen feed line. We assumed that the LNe temperature values at 0.2 MPa feeding pressure are within the range from 27 K at the feed line to 30 K at the bobbin block end connected by the return line. Here, to cool down and support the current lead, cooling anchors connect the current leads to the GNe return line. Thus, Q_l of the current leads, which can directly reduce the thermal stability of HTS coils, are absorbed by vaporized GNe flowing inside the return line pipe.

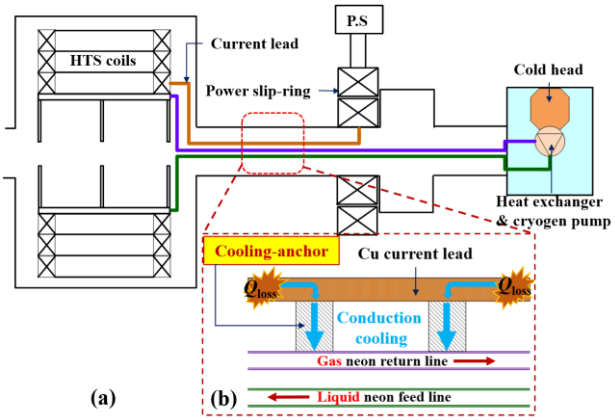

Fig. 3. (a) Basic configuration of a cryogenic cooling system and (b) conceptual design of a cooling-anchor.

2.3. The 3D Thermal FEM analysis without cooling anchor

First, for reference, we performed thermal FEM simulation without cooling anchors at the current lead to

analyze the thermal effect of Q_l on the temperature distribution in the HTS coils. As a boundary condition (BC) for the FEM analysis, the convection heat-transfer coefficients (h_c) related to forced convection were estimated based on Gnielinski correlation, which is an empirical correlation, to calculate the Nusselt number (Nu) of fully developed turbulence inside a sleek circular pipe and is expressed as [8, 9]

$$Nu = \frac{(f/8)(Re-1000)P_r}{1+12.07(f/8)^{0.5}\left(P_r^{2/3}-1\right)} \begin{bmatrix} 0.5 \le P_r \le 200 \\ 3000 \le \mathrm{Re} \le 5\times10^6 \end{bmatrix} \quad (2)$$

where, f, P_r, and Re are the friction factor which is calculated as $(0.79\ln Re\text{-}1.64)^{-2}$, the Prandtl number of the cooling fluid, and Reynolds number (Re), which is used to determine the development condition of the fluid inside the pipe, respectively.

In this calculation case, Re is 12021, which is based on 0.00525-kg/s mass flow (m) and 0.226 m/s average fluid velocity (V_m). The relationship of V_m and m is expressed as

$$m = \frac{Q}{C_p \Delta T} = \rho V_m A_c \quad (3)$$

where Q, C_p, and ΔT are the rotor heat loss, specific heat capacity of neon, and temperature difference, respectively. ρ and A_c are the LNe mass density and cross-sectional area of the cooling pipe inside, respectively.

Note that for the initial cooling system design, i.e., in case of the absence of cooling anchors, the temperature difference (ΔT) between the inlet of the cryogen feed line and outlet of the cryogen return line was designed as approximately 3 K, and all used material properties of the LNe are based on the average value at temperature range from 27 to 30 K with 0.2 MPa feeding pressure. Finally, the h_c of LNe inside the bobbin block was estimated to be 331.5 W/(m^2·K) at mean fluid temperature of 28.5 K, N_u of 30.73 from (2), and k of 0.1079 W/(m·K) for LNe.

Fig. 4 shows the thermal FEM simulation modeling with BCs considering one-sixth symmetry geometry. The heat losses of the rotor considered in this simulation have been already calculated in [2] and [3]. They are composed of radiation loss through the bobbin cover surface (Q_r), conduction loss at room temperature (300 K) through the side of the torque disk ($Q_{c.d.}$), current lead loss (Q_l), and HTS coil loss (Q_h), which accounts for the intrinsic property n-value, lap-joint, and flux-flow losses.

Table I lists the thermal conductivities in terms of the reference temperature used for the respective rotor parts in the thermal FEM simulation. In particular, the orthotropic k properties of the second-generation (2G) HTS coils with an electrical insulating layer were determined by the rule of mixtures because the tape-shaped 2G HTS wire is a composite structure consisting of various materials with different k values [10, 11]. Moreover, the Kapton and epoxy materials used for interlayer electrical insulation make heat transfer in the lamination direction of the wire difficult. Therefore, calculation of orthotropic equivalent k is required for more accurate FEM analysis. The orthotropic k values of the 2G HTS coils were estimated based on the structure design of the 2G HTS wire in [6] and [7].

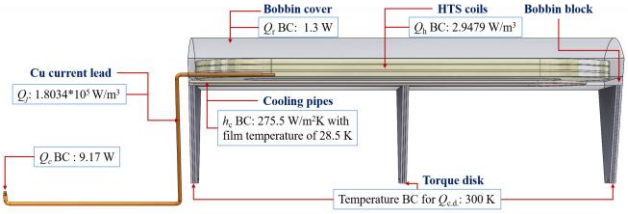

Fig. 4. Side view of analysis modeling without cooling anchors and BCs for thermal FEM simulation.

TABLE I
THERMAL CONDUCTIVITY PROPERTIES FOR FEM THERMAL ANALYSIS.

Items		Thermal conductivity [W/(m·K)]
Rotor parts	Material type	Values
HTS coil	2G HTS	Perpendicular: 0.557 at 30 K Parallel and Axial: 601 at 30 K
Bobbin block	AL6061	39.29 at 30 K
Bobbin cover	AL6061	39.29 at 30 K
Thermal plate	AL6061	39.29 at 30 K
Current lead	Copper	637 at 300-27 K†
Torque disk	G10	0.4 at 300-30 K†
Cooling pipe	SUS304	3.5 at 30 K

†: Average value in each range of temperature

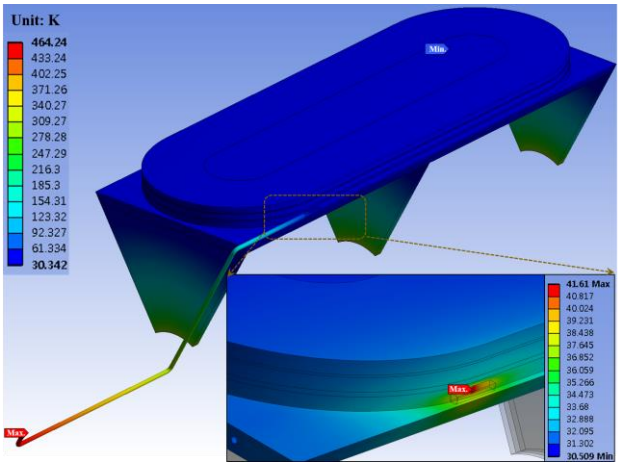

Fig. 5. Temperature distribution of rotor pole without cooling anchors.

The temperature distribution analysis without the cooling anchors was conducted with a total number of mesh elements of 1,716,561 for the one-sixth symmetry geometry. The heat losses per unit volume for the HTS coils and current lead were inputted. From the FEM simulation results, the heat loads borne by the one-sixth symmetry geometry was 4.09 W through conduction from room temperature of the G10 torque disk. The maximum temperatures were increased up to 41.61K at the junction part that joins the HTS coils to the cryogenic part of the Cu current lead and 464.24 K at room temperature in the current lead path, respectively, as shown in Fig. 5. If the HTS coils do not have sufficient thermal stability margin,

the coils cannot withstand the thermal quench because of the hot spot temperature at the junction part. Therefore, as part of thermal anchoring, a more effective cooling technique is required to keep the operating temperature of the HTS coils constant.

3. CONCEPTUAL DESIGN OF COOLING ANCHOR FOR CURRENT LEAD

3.1. Conceptual structure design of cooling anchor

Fig. 6 shows the conceptual design view of a cooling anchor with one pair of current lead and a GNe return pipe. We conceptually designed the configuration of the cooling anchor using Fourier's law; the governing equation is expressed as

$$Q_{c.a.} = \left(k(T) A_s \frac{dT}{dz} \right)\Big|_{z=l} = \left(k(T) 2\pi r_o l_c \frac{\left(T_{lead} - T_{cryogen}\right)}{l} \right) \qquad (4)$$

where $Q_{c.a.}$, A_s, r_o, and l_c are the conduction heat transferred from the current lead through the cooling anchor, conduction surface, outer radius of the cooling pipe, and axial length, respectively. T_{lead} and $T_{cryogen}$ are assumed to be the maximum temperature of the current lead along the total length and of the GNe returned to the heat exchanger in the cryostat of the external cooling system, respectively.

We considered two materials for the cooling anchors, namely, AL6061 and G10. AL6061 is a suitable candidate for a cooling anchor because it has a high thermal conductivity at cryogenic temperature and a low mass density. However, it is an electrically conductive material, which requires electric insulation between the Cu current lead and cooling anchor. Therefore, the equivalent k of AL6061 was estimated by the rule of mixtures assuming a 70-μm insulation thickness. In the G10 material case, it is a non-magnetic and non-electrically conductive material, but its thermal conductivity is extremely lower than that of AL6061. The k values applied for the cooling anchors were 17.47 and 1.75 W/(m·K) for AL6061 and G10, respectively. Finally, the dimensions of l_c corresponding to the AL6061 and G10 materials, as shown in Fig. 6 (a) were calculated by (4), and the total lengths were 29.46 and 294 mm, respectively.

3.2. The 3D thermal FEM analysis with cooling anchors

For the thermal FEM analysis with connected cooling anchors, the h_c values in the GNe return pipe were estimated by (2) and (3). *Re* in the return pipe to calculate *Nu* was 204529 based on V_m = 4.09 m/s, and its corresponding *Nu* was 279.79 with k = 0.0534 W/(m·K) for GNe. The final h_c value was estimated to be 2988 W/(m^2·K). Note that all the GNe material properties were based on the temperature range from 30 to 40 K in the return pipe, as shown in cooling path ③ in Fig. 6 (c).

Figs. 7 and 8 show the results of the temperature distribution analysis for cases with AL6061 and G10 cooling anchors, respectively. The detailed maximum and minimum temperature values are listed in Table II. In the AL6061 cooling-anchor case, the maximum temperature at the junction part was 31.317 K, which was 10.293 K (24.74 %) smaller than that without cooling anchors. For the G10 cooling-anchor case, the maximum temperature at the junction part was 31.016 K, and its value was 10.594 K (25.46 %) smaller than that without cooling anchors. We concluded that the introduction of cooling anchors is thermally effective in enhancing the HTS coil thermal stability. In other words, cooling anchors can maintain the operating temperature of HTS coils. In the comparison of the two materials for cooling anchor, the maximum temperature in the G10 case was approximately 5 K smaller than that in the AL6061 case. In conclusion, the G10

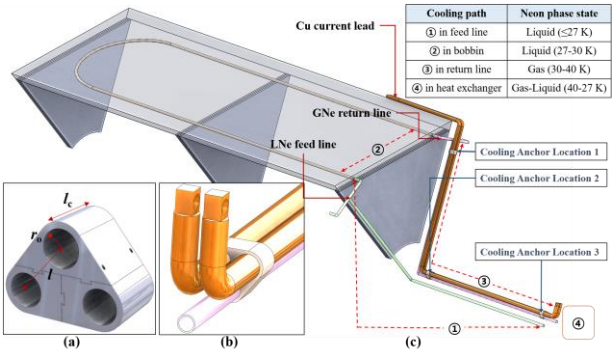

Fig. 6. Conceptual design view of (a) cooling anchor, (b) connection part, and (c) rotor cooling system structure.

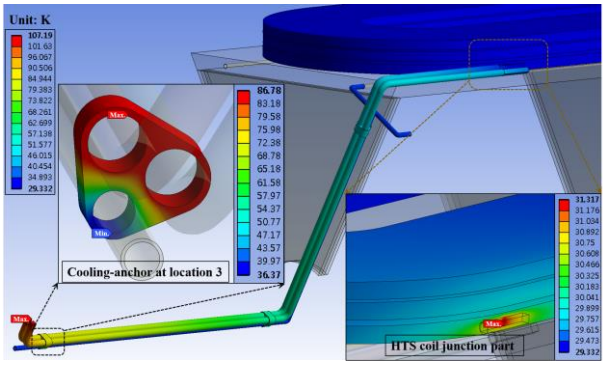

Fig. 7. Temperature distribution with AL6061 cooling anchors.

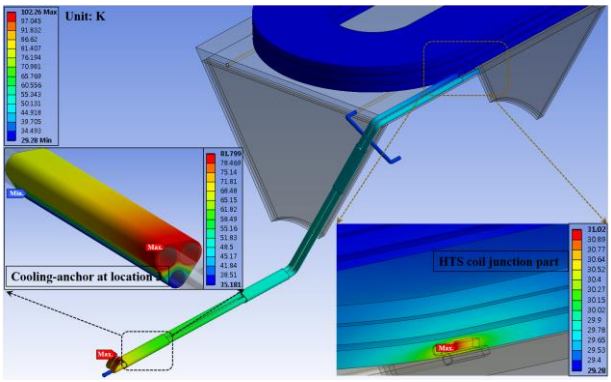

Fig. 8. Temperature distribution with G10 cooling anchors.

cooling anchor is more effective than the AL6061 case in reducing the maximum temperature at the room-temperature part of the current lead. We conclude that the contact-surface areas between the cooling anchors and lead have more effect on the current lead cooling than the cooling anchor *k* property.

3.3. Optimization design of the Cu current lead

As a part of the optimal current lead design, we considered and compared two methods. First was the recalculation of the optimal diameter of the current lead based on an existing design structure. This process can be made possible because of the changes in the temperature gradient (ΔT) between the warm and cold ends of the current lead and the material properties dependent on the temperature ranges. Second was the redesigning using division structure, which has variable d values at each appropriate temperature section, which may be expected to decrease the effect of ΔT in (1).

Table III lists the results of the optimized current lead design considering the two methods. In Method 1, the minimum Q_l values for AL6061 and G10 were 6.33 and 5.89 W, respectively. In Method 2, the Cu current lead was structurally divided into two parts with different diameters d_1 and d_2 at a specific temperature range. For the AL6061 and G10 materials, the total Q_l values with d_1 and d_2 were 7.49 and 6.64 W, respectively. By comparing the two methods, Method 1 is more suitable for minimizing Q_l than Method 2 because dividing the total length of the current lead in Method 2 resulted in the reduction in the conduction paths in the respective temperature ranges. This result definitely led to increase in Q_c, which is inversely proportional to the lead length, i.e., the conduction path, as expressed in (1). Thus, the Q_c values in Method 2 were larger than that in Method 1.

Finally, we compared the cooling load of the cryocooler without cooling anchors with that with cooling anchors, where the ΔQ_l values were used for simple comparison of the cooling loads for the respective cases listed in Table III. In conclusion, all cases listed in Table III indicated decreasing effects in terms of the cooling load of the cryocooler, and the corresponding ΔQ_l values were in the range from 10.94 to 12.54 W. The ΔQ_l value of the G10 material and Method 1 cases was smaller than those of the others conditions, and the corresponding total ΔQ_l for one pair of Cu current lead was 25.08 W. In this case, the ΔQ_l value was reduced by 68% compared with that without cooling anchors.

TABLE II
ANALYSIS RESULTS OF THE TEMPERATURE DISTRIBUTION FOR CASES WITH COOLING ANCHORS CONSIDERING VARIOUS MATERIALS.

Material type		AL6061	G10
Parts	Unit	Maximum/Minimum Temperature	
Location 1†	K	49.956/35.383	47.896/35.067
Location 2†		60.474/35.644	55.398/35.108
Location 3†		86.781/36.37	81.799/35.181
HTS coils		31.317/29.332	31.016/29.28
Current lead		107.19/30.68	102.26/30.457
Return pipe		63.08/35	49.068/35

†: locations of cooling anchors

TABLE III
COMPARATIVE RESULTS OF THE COOLING LOAD CALCULATIONS FOR THE OPTIMAL DESIGN CASES.

Material type		AL6061		G10	
Items	Unit	Method 1†	Method 2## d_1/d_2	Method 1‡	Method 2### d_1/d_2
d	mm	8.7	7.8/5.3	8.6	7/5
Q_c	W	3.18	2.59/1.16	2.98	2.48/0.81
Q_j	W	3.15	2.6/1.14	2.91	2.55/0.80
Q_l	W	6.33	5.19/2.3	5.89	5.03/1.61
ΔQ_l ᵗ	W	12.1 (66 %)	10.94 (59 %)	12.54 (68 %)	11.79 (64 %)

†: based from 30 to 107 K temperature range, ‡: based from 30 to 102 K temperature range, ##: based from 60 to 107 K (d_1) and 30 to 60 K (d_2) temperature ranges, ###: based from 51 to 102 K (d_1) and 30 to 51 K (d_2) temperature ranges, ᵗ: Q_l reduction compared with that shown in Fig. 1

4. CONCLUSIONS

In this paper, the structure of a cooling anchor for cooling performance enhancement of a Cu current lead for a 1.5-MW-class HTSSM has been conceptually designed and analyzed using 3D electromagnetic and thermal FEM software. The benefits of the cooling anchor are the reduction in the cooling load of the cryocooler and enhancement of the HTS coil thermal stability. The effects of introducing cooling anchors on the current lead cooling were confirmed by thermal FEM analysis. In conclusion, cooling anchors using AL6061 and G10 material displayed a positive effect on the cooling current lead as well as in reducing the cooling load of the cryocooler. For the optimized Cu current lead designs listed in Table III, the use of G10 material for cooling anchors and Method 1 is strongly recommended for the metal current lead design for a 1.5-MW-class HTSSM because it exhibited the largest reduction in Q_l compared with that without cooling anchors.

ACKNOWLEDGMENT

This work was supported in part by the Human Resources Program in Energy Technology of the Korea Institute of Energy Technology Evaluation and Planning (KETEP), grant funded by the Ministry of Trade, Industry & Energy, and by the National Research Foundation of Korea (NRF) grant funded by the Korea government (MSIP), Republic of Korea. (Nos. 20164030201230 and 2016R1A2B4007324)

REFERENCES

[1] T. Ge *et al.*, "Hybrid current lead design of HTS SMES," *Physics Procedia*, vol. 45, pp. 309-312, 2013.
[2] T. D. Le *et al.*, "Design of indirect closed-cycle cooling scheme coupled with a cryocooler for a 3-MW-class high-temperature

superconducting synchronous motor," *IEEE Trans. Appl. Supercond.*, vol. 26, no. 4, 2016, Art. ID. 5204904.

[3] T. D. Le *et al.*, "A compactly integrated cooling system of a combination dual 1.5-MW HTS motors for electric propulsion," *Progr. Supercond. Cryogenics*, vol. 18, no. 4, pp. 25–29, 2016.

[4] M. P. Oomen *et al*., "Transposed-cable coil & saddle coils of HTS for rotating machines: Test results at 30 K," *IEEE Trans. Appl. Supercond.*, vol. 19, no. 3, pp. 1633–1638, 2009.

[5] Y. Iwasa, *Case Studies in Superconducting Magnets: Design and Operational Issues*, 2nd ed., New York, NY, USA: Springer-Verlag, 2009, pp. 274.

[6] J. H. Kim *et al.*, "Economic analysis of a 1.5-MW-class HTS synchronous machine considering various commercial 2G CC tapes," *IEEE Trans. Appl. Supercond.*, vol. 26, no. 4, 2016, Art. ID. 5206105.

[7] J. H. Kim *et al.*, "Effects of stabilizer thickness of 2G HTS wire on the design of a 1.5-MW-class HTS synchronous machine," *IEEE Trans. Appl. Supercond.*, vol. 26, no. 4, 2016, Art. ID. 5206705.

[8] F. P. Incropera, D.P. Dewitt, T. L. Bergman, and A. S. Lavine, *Fundamental of Heat and Mass Transfer*, 6th ed., Hoboken, NJ, USA: Wiley, 2007, pp. 320–440.

[9] Y. Cengel, *Heat Transfer: A Practical Approach*, 2nd ed., New York, NY, USA: McGraw-Hill, 2003, pp. 441–449.

[10] M. D. Sumption *et al.*, "Thermal diffusion and quench propagation in YBCO pancake coils wound with ZnO and Mylar insulations," *Supercond. Sci. Technol.*, vol. 23, no. 7, 2010, Art. ID. 075004.

[11] S. H. In *et al*., "Thermal and structural analysis of a cryogenic conduction cooling system for a HTS NMR magnet," *Progr. Supercond. Cryogenics*, vol. 18, no. 1, pp. 59–63, 2016.